Fast Transient Fault-Current Detection Based on PQR Transformation Technique for a Solid-State Fault Current Limiter

B. BORIBUN & T. KULWORAWANICHPONG[†]
Power and Energy Research Unit, School of Electrical Engineering,
Institute of Engineering, Suranaree University of Technology
111 University Avenue, Nakhon Ratchasima 30000, THAILAND

Abstract: - This paper describes analysis, modeling and simulation of electrical transient fault-current detection in power systems. The proposed modeling is based on simple numerical integration only, which is able to efficiently handle some sophisticated calculation. The proposed fault detector methods are sliding root mean square (SRMS) and PQR transformation technique. In this paper, an abnormal condition is situated by simply adding a fault impedance at the fault location. With the proposed methods, transient behaviors of voltages and currents can be evaluated and detected. To demonstrate the use of the proposed simulation, a simple two-bus test system was employed for test.

Key-Words: - Solid state fault current limiter, modeling, simulation, PQR, sliding RMS, transient analysis

1 Introduction

Development of electro-magnetic transient programs (EMTP) [1] for power system analysis has very long history and can be achieved in many different approaches. Some are direct but rather difficult, while some are quite simple but inaccurate. Although up-to-date commercial EMTP software is reliable and accurate to do this job, there also exist limitations in which some programming modification to enhance its ability to satisfy several aspects demanded by users is prohibited. In power system fault analysis, for example, it is very difficult to determine other quantities that are not provided by the software package, e.g. transient analysis. In addition, such commercial software is very expensive.

In this paper, derivation of electrical transient models leading to generalized algorithms to simulate an abnormal operating condition in electrical power systems and the fault detector is proposed [2]. To avoid complicated computation, simple methods are only employed. Trapezoidal integration is the main numerical technique to simplify a set of differential equations, which represent system transient behaviors [3]. Fault analysis is of interest in this paper, thus modeling and simulation described herein is particularly focused on transient fault current calculation. For any other purposes, additional modification might be required. It depends on degree of accuracy and complication of systems under consideration.

Section 2 of this paper illustrates derivation of electrical transient modeling for each individual power system component that is necessary to formulate power system fault equations. Section 3 provides two methods of fault detector during the transient situation, which is the integration of those described in Section 2. Simulation results were obtained by employing a two-bus system. The last section gives conclusion of the work.

2 Power Network Modeling

The proposed power network consists of four fundamental elements such as substation, feeder line, load, and three-phase-to ground fault. The numerical modeling for all elements is described and formulated by the nodal analysis method. The applied numerical method is trapezoidal rule. The final difference equations of models are very simple and easy to programming by any programming language [4].

2.1 Substation Modeling

The configuration of substation is shown in Fig. 1 in which consist of balance three voltage source connect any bus k. The three phase current injected bus k is given by,

$$i_{abc,g}^{(k)}(t) = G_g^{(k)}\left\{v_{abc,g}^{(k)}(t) - v_{abc,n}^{(k)}(t)\right\} \qquad (1)$$

where $v_{abc,g}^{(k)}$ and $v_{abc,g}^{(k)}$ are three phase voltage of the substation and bus k respectively. The elements of $G_g^{(k)}$ is given by,

$$\boldsymbol{G}_{g}^{(k)} = \begin{bmatrix} 1000 & 0 & 0 \\ 0 & 1000 & 0 \\ 0 & 0 & 1000 \end{bmatrix} \qquad (2)$$
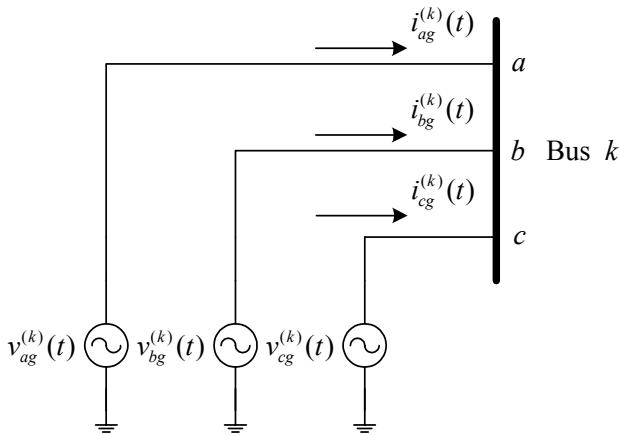
Fig. 1. Substation

2.2 Feeder Lines Modeling

The configuration of feeder line which connects bus k and bus m is shown in Fig. 2.
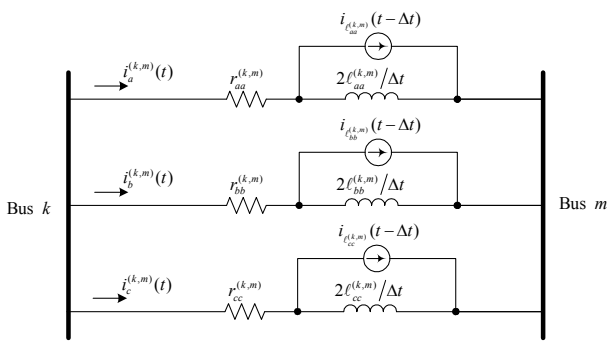
Fig. 2. Feeder line

The three phase current inject from bus k to bus m is given by,

$$\begin{aligned} \boldsymbol{i}_{abc}^{(k,m)}(t) &= \boldsymbol{G}_{abc}^{(k,m)}\left(\boldsymbol{v}_{abc,n}^{(k)}(t) - \boldsymbol{v}_{abc,n}^{(m)}(t)\right) \\ &+ \boldsymbol{K}_{abc}^{(k,m)}\boldsymbol{i}_{abc,\ell}^{(k,m)}(t - \Delta t) \end{aligned} \qquad (3)$$

where Δt is the time step of simulation. The elements of $\boldsymbol{G}_{abc}^{(k,m)}$ and $\boldsymbol{K}_{abc}^{(k,m)}$ are given by Eq. (4) and Eq. (5) respectively.

$$\boldsymbol{G}_{abc}^{(k,m)} = \begin{bmatrix} \dfrac{1}{r_{aa}^{(k,m)} + 2\ell_{aa}^{(k,m)}/\Delta t} & 0 & 0 \\ 0 & \dfrac{1}{r_{bb}^{(k,m)} + 2\ell_{bb}^{(k,m)}/\Delta t} & 0 \\ 0 & 0 & \dfrac{1}{r_{aa}^{(k,m)} + 2\ell_{aa}^{(k,m)}/\Delta t} \end{bmatrix} \qquad (4)$$

$$\boldsymbol{K}_{abc}^{(k,m)} = \begin{bmatrix} \dfrac{2\ell_{aa}^{(k,m)}}{\Delta t r_{aa}^{(k,m)} + 2\ell_{aa}^{(k,m)}} & 0 & 0 \\ 0 & \dfrac{2\ell_{bb}^{(k,m)}}{\Delta t r_{bb}^{(k,m)} + 2\ell_{bb}^{(k,m)}} & 0 \\ 0 & 0 & \dfrac{2\ell_{cc}^{(k,m)}}{\Delta t r_{cc}^{(k,m)} + 2\ell_{cc}^{(k,m)}} \end{bmatrix} \qquad (5)$$

The induced three phase current of feeder line inductors is given by,

$$\begin{aligned} \boldsymbol{i}_{abc,\ell}^{(k,m)}(t) &= \boldsymbol{i}_{abc,\ell}^{(k,m)}(t - \Delta t) + \boldsymbol{K}_{abc,\ell}^{(k,m)}\boldsymbol{i}_{abc,\ell}^{(k,m)}(t - \Delta t) \\ &+ \boldsymbol{G}_{abc,\ell}^{(k,m)}\left(\boldsymbol{v}_{abc,n}^{(k)}(t - \Delta t) - \boldsymbol{v}_{abc,n}^{(m)}(t - \Delta t)\right) \end{aligned} \qquad (6)$$

The elements of $\boldsymbol{G}_{abc,\ell}^{(k,m)}$ and $\boldsymbol{K}_{abc,\ell}^{(k,m)}$ are given by Eq. (7) and Eq. (8) respectively.

$$\boldsymbol{G}_{abc,\ell}^{(k,m)} = \begin{bmatrix} \dfrac{\Delta t}{2\ell_{aa}^{(k,m)}} & 0 & 0 \\ 0 & \dfrac{\Delta t}{2\ell_{bb}^{(k,m)}} & 0 \\ 0 & 0 & \dfrac{\Delta t}{2\ell_{bb}^{(k,m)}} \end{bmatrix} \qquad (7)$$

$$\boldsymbol{K}_{abc,\ell}^{(k,m)} = \begin{bmatrix} \dfrac{\Delta t r_{aa}^{(k,m)}}{2\ell_{aa}^{(k,m)}} & 0 & 0 \\ 0 & \dfrac{\Delta t r_{bb}^{(k,m)}}{2\ell_{bb}^{(k,m)}} & 0 \\ 0 & 0 & \dfrac{\Delta t r_{cc}^{(k,m)}}{2\ell_{cc}^{(k,m)}} \end{bmatrix} \qquad (8)$$

2.3 Load Modeling

The configuration of load connects bus k shown in Fig. 3. The proposed load model is consisting of resistor and inductor which the connection is parallel.
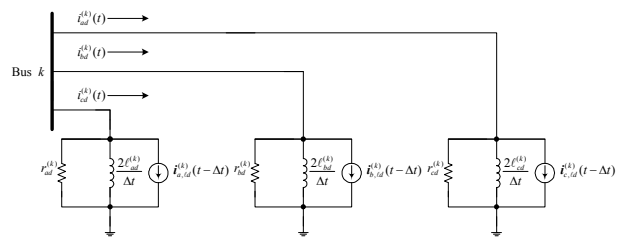
Fig. 3. Shunt resistor and inductor load

The three phase current which bus k supply to load is given by,

$$\boldsymbol{i}_{abc,d}^{(k)}(t) = \boldsymbol{G}_{abc,d}^{(k)} \boldsymbol{v}_{abc,n}^{(k)}(t) + \boldsymbol{i}_{abc,\ell d}^{(k)}(t - \Delta t) \quad (9)$$

The elements of $\boldsymbol{G}_{abc,d}^{(k)}$ is given by Eq. (10).

$$\boldsymbol{G}_{abc,d}^{(k,m)} = \begin{bmatrix} \dfrac{2r_{ad}^{(k)}\ell_{ad}^{(k)}}{\Delta t r_{ad}^{(k)} + 2\ell_{ad}^{(k)}} & 0 & 0 \\ 0 & \dfrac{2r_{cd}^{(k)}\ell_{cd}^{(k)}}{\Delta t r_{cd}^{(k)} + 2\ell_{cd}^{(k)}} & 0 \\ 0 & 0 & \dfrac{2r_{cd}^{(k)}\ell_{cd}^{(k)}}{\Delta t r_{cd}^{(k)} + 2\ell_{cd}^{(k)}} \end{bmatrix} \quad (10)$$

The induced three phase load current is given by,

$$\boldsymbol{i}_{abc,\ell d}^{(k)}(t) = \boldsymbol{i}_{abc,\ell d}^{(k)}(t - \Delta t) + \boldsymbol{G}_{abc,\ell d}^{(k)} \boldsymbol{v}_{abc,n}^{(k)}(t) \quad (11)$$

The elements of $\boldsymbol{G}_{abc,\ell d}^{(k)}$ is given by,

$$\boldsymbol{G}_{abc,\ell d}^{(k)} = \begin{bmatrix} \dfrac{\Delta t}{2\ell_{ad}^{(k)}} & 0 & 0 \\ 0 & \dfrac{\Delta t}{2\ell_{bd}^{(k)}} & 0 \\ 0 & 0 & \dfrac{\Delta t}{2\ell_{vd}^{(k)}} \end{bmatrix} \quad (12)$$

2.4 Three Phase Fault Modeling

This paper is only proposed the three-phase-to-ground fault case. The configuration model is shown in Fig. 4.
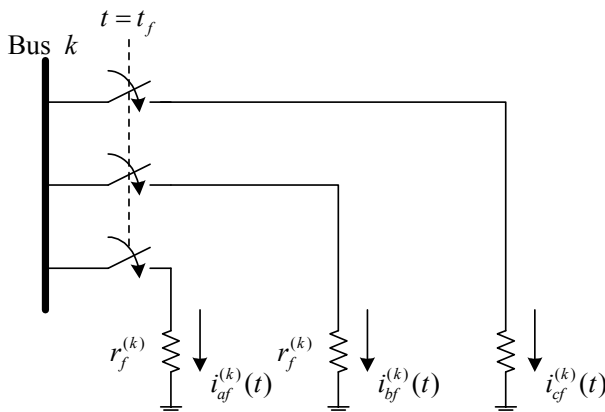
Fig. 4. Three-phase-to-ground fault

The three phase fault current is given by,

$$\begin{bmatrix} i_{af}^{(k)}(t) \\ i_{bf}^{(k)}(t) \\ i_{cf}^{(k)}(t) \end{bmatrix} = \begin{bmatrix} 1/r_f^{(k)} & 0 & 0 \\ 0 & 1/r_f^{(k)} & 0 \\ 0 & 0 & 1/r_f^{(k)} \end{bmatrix} \begin{bmatrix} v_{an}^{(k)}(t) \\ v_{bn}^{(k)}(t) \\ v_{cn}^{(k)}(t) \end{bmatrix} \quad (12)$$

2.5 Solid-State Fault Current Limiter

The general configuration of the SSFCL [5-7] is shown in Fig. 5. The two lower GTOs are switches for forward and reverse feeder line current which flowing between source side and load side. The two upper GTOs are switches for control the connection of FCL. The FCL is connected in parallel the feeder line corresponding to the command of fault detector. During fault, feeder line is isolated from the system while FCL will connect the source side and load side. Because of the high impedance of inductor FCL, the fault current is decrease and the reliability of system is improved.
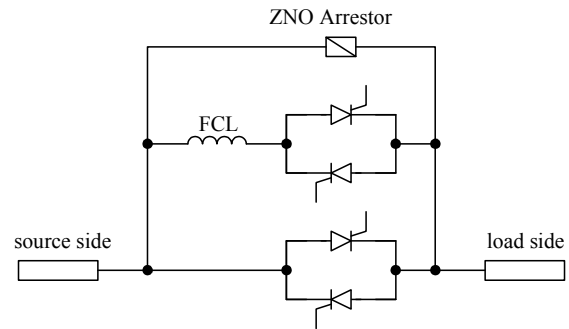
Fig. 5. Fault current limiter

The simple simulation model of FCL of proposed paper is shown in Fig. 6.
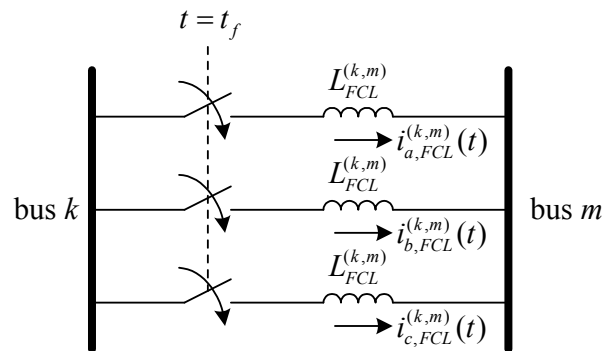
Fig. 6. Fault current limiter

This model is similar to the feeder line model which removed resistors. The three phase current of FCL which connect bus k and bus m is given by,

$$\boldsymbol{i}_{FCL}^{(k,m)}(t) = \boldsymbol{i}_{FCL}^{(k,m)}(t-\Delta t)$$
$$+ \boldsymbol{G}_{FCL}^{(k,m)}\left(\boldsymbol{v}_{abc,n}^{(k)}(t) - \boldsymbol{v}_{abc,n}^{(m)}(t)\right) \qquad (13)$$
$$+ \boldsymbol{G}_{FCL}^{(k,m)}\left(\boldsymbol{v}_{abc,n}^{(k)}(t-\Delta t) - \boldsymbol{v}_{abc,n}^{(m)}(t-\Delta t)\right)$$

The elements of $\boldsymbol{G}_{abc,\ell d}^{(k)}$ is given by,

$$\boldsymbol{G}_{abc,\ell d}^{(k)} = \begin{bmatrix} \dfrac{\Delta t}{2L_{FCL}^{(k,m)}} & 0 & 0 \\[3mm] 0 & \dfrac{\Delta t}{2L_{FCL}^{(k,m)}} & 0 \\[3mm] 0 & 0 & \dfrac{\Delta t}{2L_{FCL}^{(k,m)}} \end{bmatrix} \qquad (14)$$

3 Transient Analysis

The configuration of over all system of power network is shown in Fig. 7.
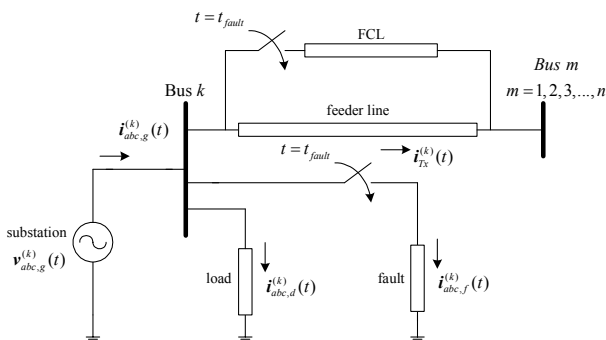
Fig. 7 The power network

When consider over all system at bus k, the total sum of all currents must be zero and equal to summation of equations (1), (3), (9), (12),and (13). The final form of system current equation can be rearranged to be simple as equation (15).

$$-\sum_{m=1}^{k-1}\left(\left(\boldsymbol{G}_{abc}^{(k,m)} + \boldsymbol{G}_{abcFCL}^{(k)}\right)\boldsymbol{v}_{abc,n}^{(m)}(t)\right)$$
$$+\left(\boldsymbol{G}_g^{(k)} + \boldsymbol{G}_{abc}^{(k,m)} + \boldsymbol{G}_{abcF}^{(k)} + \boldsymbol{G}_{abcFCL}^{(k)}\right)\boldsymbol{v}_{abc,n}^{(k)}(t)$$
$$-\sum_{m=k+1}^{n}\left(\left(\boldsymbol{G}_{abc}^{(k,m)} + \boldsymbol{G}_{abcFCL}^{(k)}\right)\boldsymbol{v}_{abc,n}^{(m)}(t)\right) \qquad (15)$$
$$=$$
$$\boldsymbol{G}_g^{(k)}\boldsymbol{v}_{abc,g}^{(k)}(t) - \boldsymbol{i}_{abc,\ell d}^{(k)}(t-\Delta t) - \boldsymbol{K}_{abc}^{(k,m)}\boldsymbol{i}_{abc,\ell}^{(k,m)}(t-\Delta t)$$

With N buses corresponding to N independent variables, the compact matrix of equation (13) can be formed as,

$$\boldsymbol{G}\boldsymbol{v}_{abc}(t) = \boldsymbol{i}_{abc}^{(k)}(t) \qquad (16)$$

where $\boldsymbol{G}$ is the conductance matrix, $v_{abc}(t)$ is the bus voltage vector, and $\boldsymbol{i}_{abc}^{(k)}(t)$ is the bus current vector. Elements of the matrix $\boldsymbol{G}$ can be computed by using the following expressions,

$$\boldsymbol{g}_{abc}^{(k,m)} = -\left(\boldsymbol{G}_{abc}^{(k,m)} + \boldsymbol{G}_{abcFCL}^{(k)}\right) \qquad ,k \neq m$$
$$\boldsymbol{g}_{abc}^{(k,k)} = \boldsymbol{G}_g^{(k)} + \boldsymbol{G}_{abc}^{(k,m)} + \boldsymbol{G}_{abcF}^{(k)} + \boldsymbol{G}_{abcFCL}^{(k)} \qquad ,k = m \qquad (17)$$

As can be seen, the bus voltage can be obtained by solving equation (16) and other variables can be calculated by their equations which related to bus voltage.

4 Fault Detection Techniques

There are various fault detection methods. This paper proposed the simple technique called sliding root mean square (SRMS) method and novel technique called PQR transformation [8,9]. The SRMS method is the normal detection of analog meter while the PQR transformation needs more measurement tools and computation. The SRMS can be computed by using the following expressions,

$$X_{RMS} = \sqrt{\dfrac{1}{N-1}\sum_{k=1}^{N} X^2(k)} \qquad (18)$$

where k is the sampling number of X and $N-1$ is the sampling period. The evaluation of PQR domain can be computed by,

$$\begin{bmatrix} i_p \\ i_q \\ i_r \end{bmatrix} = \boldsymbol{C}\begin{bmatrix} i_a \\ i_b \\ i_c \end{bmatrix} \qquad (19)$$

where $\boldsymbol{C}$ is given by,

$$\boldsymbol{C} = \dfrac{\sqrt{2}}{3}\boldsymbol{C}_{reff}\begin{bmatrix} 1/\sqrt{2} & 1/\sqrt{2} & 1/\sqrt{2} \\ 1 & -1/2 & -1/2 \\ 0 & \sqrt{3}/2 & -\sqrt{3}/2 \end{bmatrix} \qquad (20)$$

$$C_{reff} = \begin{bmatrix} 0 & i_{areff}/i_{\alpha\beta reff} & i_{\beta reff}/i_{\alpha\beta reff} \\ 0 & -i_{\beta reff}/i_{\alpha\beta reff} & i_{\alpha reff}/i_{\alpha\beta reff} \\ 1 & 0 & 0 \end{bmatrix} \quad (21)$$

$$\begin{bmatrix} i_{\alpha reff} \\ i_{\beta reff} \end{bmatrix} = \frac{\sqrt{2}}{3} \begin{bmatrix} 1 & -1/2 & -1/2 \\ 0 & \sqrt{3}/2 & -\sqrt{3}/2 \end{bmatrix} \begin{bmatrix} i_{areff} \\ i_{breff} \\ i_{creff} \end{bmatrix} \quad (22)$$

$$i_{\alpha\beta reff} = \sqrt{i_{\alpha reff}^2 + i_{\beta reff}^2} \quad (23)$$

where i_{areff}, i_{breff}, and i_{creff} are the balanced three phase voltage reference which the selection should be optimized both of magnitude and phase.

5 Simulation Results

To evaluate the performance of the proposed simulation technique with balanced three-phase system, a 6-MA, 22-kV, 50 Hz, 2-bus power system was tested as shown in Fig. 8.
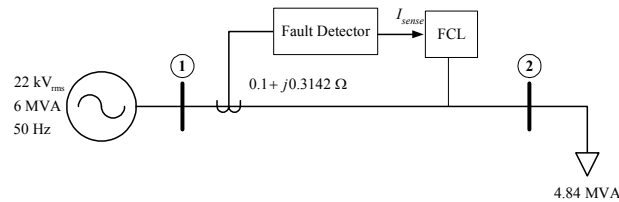
Fig. 8 The power network

The simulation situated the thee-phase-to-ground fault at bus 2. The three fault resistance of the test was 0.1 Ohms. This abnormal condition was applied in a time interval of 0.10-0.2 s. Fig. 9 presents the simulated PQR value of fault current. Fig. 10 presents the comparing of the speed of RMS and PQR fault detector while Fig. 11 is the zoom view.
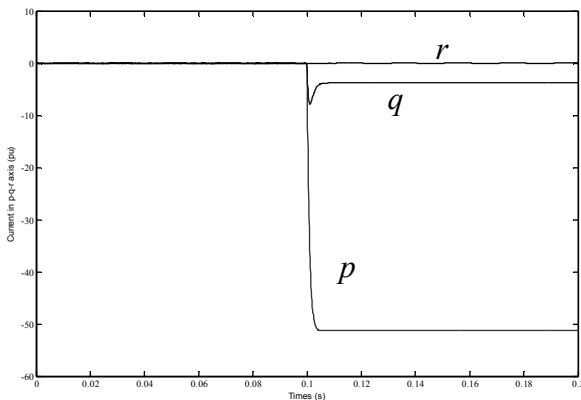
Fig. 9 The PQR thee-phase-to-ground fault current
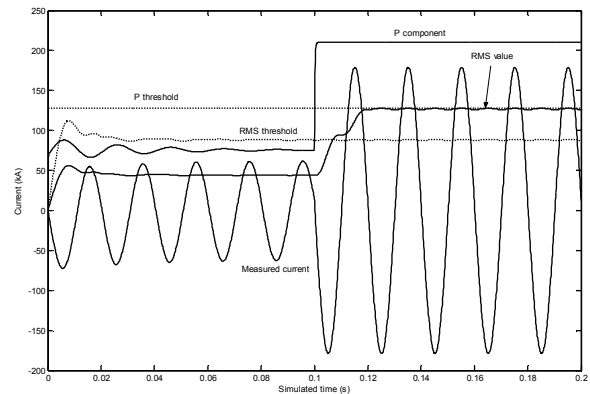
Fig. 10 The comparison of PQR and RMS method
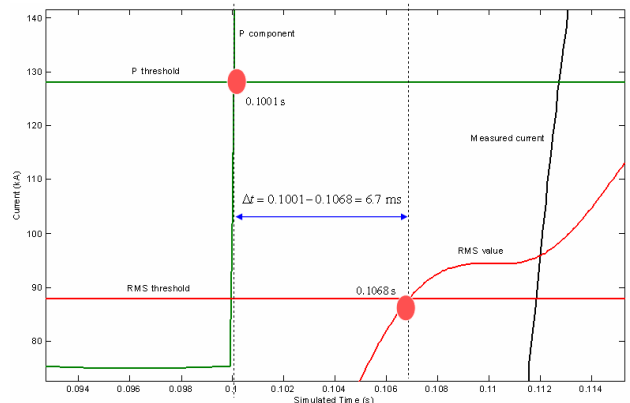
Fig. 11 The zoom view of Fig. 10
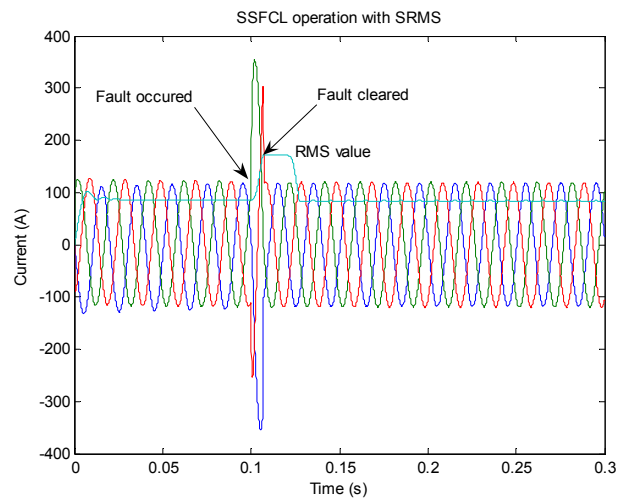
Fig. 12 Time domain response based on SRMS detection

The line of P-threshold is the maximum P-current which the diagnosis of fault detector is decided while the RMS method employed the RMS-threshold. The P-current cut the P-threshold at $t = 100.1$ ms while the cutting point of RMS-current was $t = 106.8$ ms. According to these simulation

results, it is clear that the speed of PQR-detector is faster than RMS-detector which the difference time speed was equal to $0.1067 - 0.1001 = 6.7$ ms. The current response is also shown in Fig.12.

6 Conclusion

This paper proposes electrical transient modeling for power system fault analysis with SSFCL and fault detector. It is based on simple numerical integration. In this paper, an abnormal condition is situated by simply adding a fault resistance at the fault location while the SSFCL is situated by adding inductor in between any two buses. With the proposed methods, transient behaviors of voltages and currents can be quickly detected and therefore to give fast response to connect the FCL into the system. The fast fault current detection can be achieved by using PQR transformation. The effectiveness of the proposed simulation is verified via the two-bus test power system. As a result, the proposed simulation shows that the PQR has ability to detect occurrence of fault rapidly and faster than the SRMS.

References:
[1] Ibrahim, A., Dommel, H.W., Niimura, T., *Transmission line model for large step size transient simulation*, Proc. IEEE Conf. on Electrical and Computer Engineering, Canada, pp.1191-1194, 1999.
[2] Arrillaga, J. Watson, N.R., *Computer Modeling of Electric Power Systems*. John Wiley and Sons, 2001,
[3] Part-Enander, E., Sjoberg, A., *The MATLAB 5 Handbook*, Addison-Wesley, 1999.
[4] Borriboon, B., Oonsivilai, A., Kulworawanichpong, T., *Electrical transient modeling for power system fault simulation*, International Conference on Electrical, Electronics, Computer, Telecommunications and Information Technology (ECTI 2005), Pattaya, Thailand, 12 – 13 May 2005
[5] Ahmed, M.M.R., Putrus, G. A.; Ran, L. Xiao, L. *Harmonic analysis and improvement of new solid-state fault current limiter*. IEEE Transactions on Industry Applications, Vol. 40, pp. 1012-1019, 2004
[6] Chen; G., Jiang; D., Lu; Z., and Wu, Z., *A new proposal for solid state fault current limiter and its control strategies,* IEEE Power Engineering Society General Meeting, Vol. 2, pp. 1468 – 1473, 2004
[7] Hannan, M.A., Mohamed, A., *Performance evaluation of solid state fault current limiters in electric distribution system*, Proceedings Student Conference on Research and Development, pp. 245 – 250, 2003
[8] Kim, H., Ji, J.K., Kim, J.H., Sul, S.K., Kim, K.H., *Novel topology of a line interactive UPS using PQR instantaneous power theory,* The 39th IAS Annual Meeting Conference Record of the 2004 IEEE Industry Applications Conference, Vol. 4, pp.2232 – 2238, 2004
[9] Lee, S.J., Kim, H., Sul, K.S., Blaabjerg, F., *A novel control algorithm for static series compensators by use of PQR instantaneous power theory*, IEEE Transactions on Power Electronics, Vol. 19, pp. 814 – 827, 2004